

Discovery of Iodinated Somatostatin Analogues Selective for *hsst2* and *hsst5* with Excellent Inhibition of Growth Hormone and Prolactin Release from Rat Pituitary Cells[†]

Sandra Blaj Moore,[‡] Joost van der Hoek,[§] Antonia de Capua,[‡] Peter M. van Koetsveld,[§] Leo J. Hofland,[§] Steven W. J. Lamberts,[§] and Murray Goodman^{*,‡}

University of California—San Diego, 9500 Gilman Drive, La Jolla, California 92093-0343, and Erasmus MC, Rotterdam, The Netherlands

Received April 21, 2005

Inhibition of growth hormone (GH) and prolactin (PRL) release from the anterior pituitary gland is mediated through somatostatin receptor subtypes *sst2* and *sst5*. It has been found that somatostatin (SS) analogues that are selective for both receptor subtypes are more effective at inhibiting GH and PRL release than monospecific analogues alone. We synthesized several disulfide-bridged octapeptide SS analogues. Iodinated compounds **7**, (4-amino-3-iodo)-D-Phe-c[Cys-Tyr-D-Trp-Lys-Val-Cys]-Thr-NH₂, and **9**, (4-amino-3-iodo)-D-Phe-c[Cys-(3-iodo)-Tyr-D-Trp-Lys-Val-Cys]-Thr-NH₂, were as potent as somatostatin in binding at receptors *hsst2* and *hsst5* and inhibited GH and PRL release from rat pituitary cells as potently as somatostatin.

Introduction

Somatostatin (somatotropin release-inhibiting factor or SRIF, as initially named) is an important regulatory peptide hormone isolated in 1973 as a factor responsible for inhibiting growth hormone release.¹ There are two forms of native somatostatin: SS-14, with 14 amino acids, and SS-28, extended at the N-terminus.² The hormone is expressed in the central and peripheral nervous systems and various organs, especially in the gastrointestinal tract. It inhibits the secretion of growth hormone (GH), thyroid stimulating hormone (TSH), and prolactin (PRL) from the anterior pituitary gland and reduces the release of insulin and glucagon from the pancreas.^{1,3–6} Somatostatin's biological actions are mediated through five G-protein-coupled receptors.^{7–10} The receptors have been cloned and characterized in the early 1990s, and much research ensued to determine the functions arising from interaction of somatostatin with each individual receptor subtype. (Notations: SST, endogenous receptors; *sst*, cloned receptors; *hsst2*, cloned human somatostatin receptor subtype 2.) This interest stemmed from the biological actions of somatostatin. Because the hormone inhibits GH release, its potential for treating cancers and other diseases characterized by excessive growth, such as acromegaly and diabetic retinopathy, became attractive. However, from the clinical point of view, the use of the natural hormone is hampered by disadvantages such as a very short half-life in the blood and the necessity for intravenous administration. Over the years, much research has been carried out to obtain analogues that are smaller and show increased resistance to the action of enzymes.

Somatostatin receptors are expressed in a variety of human tumors, such as pituitary tumors, endocrine

pancreatic tumors, carcinoids, paragangliomas, small-cell lung cancers, medullary thyroid carcinomas, pheochromocytomas, meningiomas, astrocytomas, neuroblastomas, and some breast cancers.¹¹ Usually, several subtypes of receptors are overexpressed by these tumors.

After binding of ligands to somatostatin receptors, the agonist–receptor complexes are internalized by cells. This property is important practically and constitutes the basis of localization and treatment of tumors that overexpress somatostatin receptors with radiolabeled somatostatin agonists.¹²

GH-secreting adenomas and prolactinomas are the most common functioning pituitary adenomas (tumors). It was revealed that both *hsst2* and *hsst5* mRNA were expressed in primary human fetal pituitary cells.¹³ Growth hormone secretion was suppressed equally well by analogues selective for *hsst2* or *hsst5*. Prolactin was inhibited by compounds selective for *hsst2*. It was therefore concluded that SRIF regulation of GH is mediated by both *hsst2* and *hsst5* in human fetal pituitary cells. In further experiments,¹⁴ the authors tested the effect of various receptor-selective analogues upon inhibition of GH and PRL secretion from primary human GH- and PRL-secreting pituitary adenoma cultures. It was confirmed that both *hsst2* and *hsst5* are involved in GH regulation from these adenomas. Indeed, analogue combinations containing both *hsst2* and *hsst5* selective compounds were more potent in decreasing GH than monospecific analogues used alone.

On the basis of these studies, other researchers investigated the effects of *hsst2*, *hsst5*, or *hsst2* and *hsst5* selective analogues upon inhibition of GH and PRL from GH-secreting adenomas and mixed GH–PRL adenomas.¹⁵ The GH-secreting tumors investigated, collected from acromegalic patients, were classified as either “full responders to octreotide” or “partially sensitive to octreotide”. It was shown that in all cases, but especially in the “partial responders”, a biselective

[†] This article is published in the memory of Professor Murray Goodman.

^{*} On behalf of Professor Goodman, all correspondence should be directed to Joseph P. Taulane. Phone: 858-534-4801. Fax: 858-534-0202. E-mail: jpt@chem.ucsd.edu.

[‡] University of California—San Diego.

[§] Erasmus MC.

Table 1. Compounds Reported^a

number	compound
1	D-Phe-c[Cys-Tyr-D-Trp-Lys-Val-Cys]-Asp-NH ₂
2	(4-amino)-D-Phe-c[Cys-Tyr-D-Trp-Lys-Val-Cys]-Thr-NH ₂
3	(4-amino)-D-Phe-c[Cys-Tyr-D-Trp-Lys-Val-Cys]-Asp-NH ₂
4	(4-amino)-D-Phe-c[Cys-Tyr-D-Trp-Lys-Val-Cys]-D-Thr-NH ₂
5	(4-amino)-D-Phe-c[Cys-Tyr-D-Trp-Lys-Val-Cys]-D-Asp-NH ₂
6	(4-amino)-D-Phe-c[Cys-(3-iodo)-Tyr-D-Trp-Lys-Val-Cys]-Thr-NH ₂
7	(4-amino-3-iodo)-D-Phe-c[Cys-Tyr-D-Trp-Lys-Val-Cys]-Thr-NH ₂
8	(4-amino-3-iodo)-D-Phe-c[Cys-Tyr-D-Trp-Lys-Val-Cys]-Asp-NH ₂
9	(4-amino-3-iodo)-D-Phe-c[Cys-(3-iodo)-Tyr-D-Trp-Lys-Val-Cys]-Thr-NH ₂
10	(4-amino-3-iodo)-D-Phe-c[Cys-(3-iodo)-Tyr-D-Trp-Lys-Val-Cys]-Asp-NH ₂

^a The analytical data are shown in the Experimental Section.

analogue for both *hsst2* and *hsst5* was more effective in suppressing GH and PRL than either *hsst2* or *hsst5* selective analogues alone. This finding is significant, since 40–50% of acromegaly patients are partially or poorly controlled by current somatostatin analogue therapy (see also Freda et al.¹⁶).

Somatostatin analogues have been used in the treatment of acromegaly and gastroenteropancreatic (GEP) tumors. They are well tolerated compared to other antineoplastic therapies because their side effects are minor and transient, disappearing after 2 weeks of treatment.¹⁷ Even though a relatively rare disease, acromegaly is difficult to treat, and new somatostatin analogues selective for *hsst2* and *hsst5* receptors are promising candidates for therapy. Prolactinomas are another kind of neuroendocrine tumor, which are difficult to treat. Generally, PRL hypersecretion can be controlled with dopamine (DA) agonists in about 70% of patients.¹⁸ Patients who exhibit resistance or DA agonist intolerance would benefit greatly from novel *hsst2* and *hsst5* receptor selective somatostatin analogues.

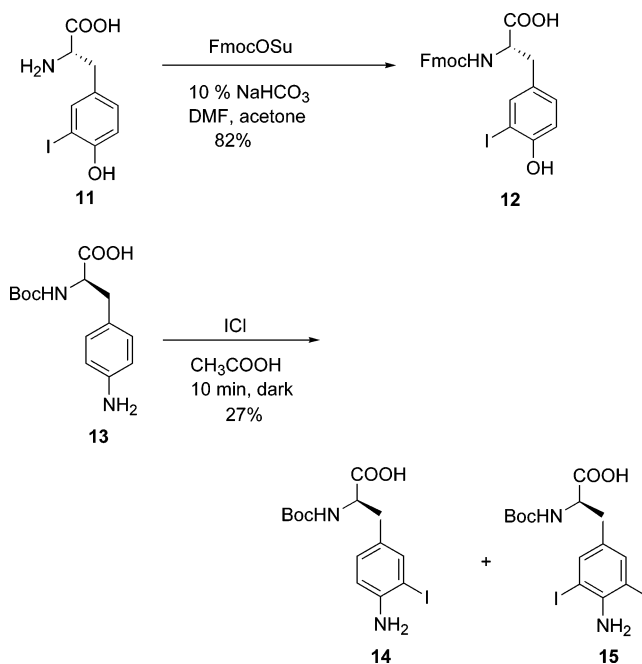
Even though *sst* selective peptide and non-peptide analogues have been discovered,¹⁹ there is a need for potent and selective ligands, amenable to radioiodination, to gain a better understanding of the physiological role of somatostatin and its individual receptors and to provide useful clinical tools. We focused on achieving SS analogues with selectivity at the *hsst2* and *hsst5* receptors, to be used for the detection and treatment of cancers, acromegaly, prolactinomas, and diabetic retinopathy.

Results

Synthesis. We synthesized a series of disulfide-bridged octapeptides incorporating non-natural amino acid building blocks. The peptide structures are shown in Table 1. One of the building blocks used was Boc-(4-Fmoc-amino)-D-Phe-OH (commercially available). For the series of iodinated peptides, we sought methods to obtain monoiodinated peptidomimetic building blocks, Fmoc-(3-iodo)-Tyr-OH [i.e., (*S*)-(fluorenylmethoxycarbonyl)-2-amino-3-(4-hydroxy-3-iodophenyl)propanoic acid] and Boc-(4-amino-3-iodo)-D-Phe-OH [i.e., (*R*)-(tert-butyloxycarbonyl)-2-amino-3-(4-amino-3-iodophenyl)propanoic acid] with the main chain amine appropriately protected with Fmoc or Boc.

The syntheses of the iodinated building blocks are illustrated in Scheme 1. The peptidomimetic amino acid Fmoc-(3-iodo)-tyrosine (**12**) was obtained by Fmoc protection of commercially available *H*-(3-iodo)-tyrosine [(3-*I*)-L-Tyr, **11**], in the presence of 10% NaHCO₃ overnight.

Scheme 1. Synthesis of Building Blocks Fmoc-(3-iodo)-Tyr-OH (**12**) and Boc-(4-amino-3-iodo)-D-Phe-OH (**14**)



The amino acid Boc-(4-amino-3-iodo)-D-Phe-OH (**14**) resulted by reaction of Boc-(4-amino)-D-Phe-OH (**13**) with ICl in glacial acetic acid for 10 min in the dark (Scheme 1). The following protected amino acids were used: Fmoc-Thr(*t*Bu)-OH, Fmoc-Asp(*O**t*Bu)-OH, Fmoc-Cys(Acm)-OH, Fmoc-Val-OH, Fmoc-Lys(Boc)-OH, Fmoc-D-Trp(Boc)-OH, Fmoc-Tyr(*t*Bu)-OH, Boc-D-Phe-OH, Boc-(4-Fmoc-amino)-D-Phe-OH and the unusual iodinated amino acids Fmoc-(3-iodo)-Tyr-OH (**12**) and Boc-(4-amino-3-iodo)-D-Phe-OH (**14**), prepared as described above. Coupling reagents used included PyBOP or HBTU in combination with HOBt and DIEA.

The peptide amides were constructed on Rink amide MBHA resin by Fmoc/*tert*-butyl protocols, cyclized via disulfide bridges on the resin using excess iodine in DMF and cleaved from the resin with 95% TFA. The crude peptides were lyophilized and purified by RP-HPLC. The syntheses were not optimized for yields. Scheme 2 illustrates the synthesis of peptide **9**, (4-amino-3-iodo)-D-Phe-c[Cys-(3-iodo)-Tyr-D-Trp-Lys-Val-Cys]-Thr-NH₂ (Figure 1). Fmoc-(3-*I*)-Tyr-OH was coupled overnight using the same coupling mixture as for building the peptide chain, PyBOP/HOBt/DIEA in DMF (4:2:8 equiv to the theoretical maximal loading on the resin). The last amino acid, Boc-(4-amino-3-iodo)-D-Phe-

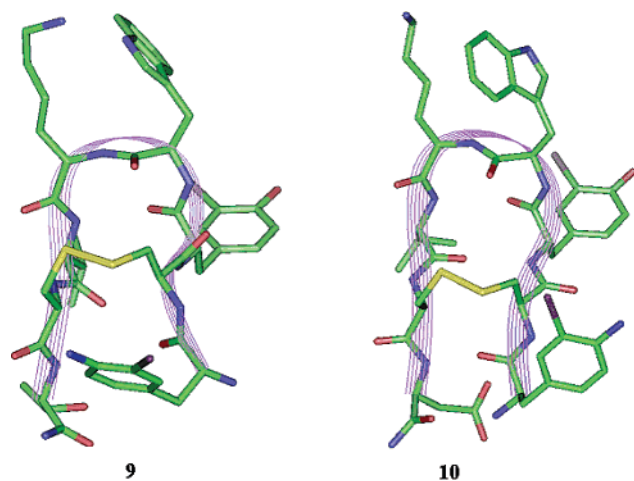
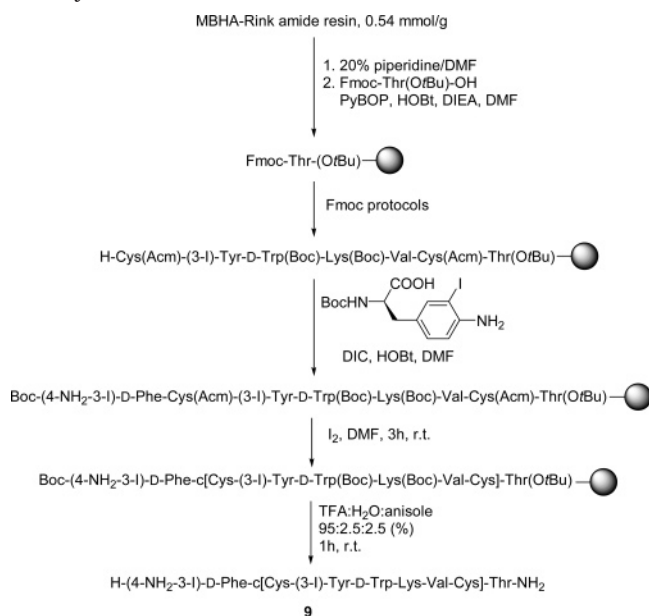


Figure 1. Preferred conformational clusters for compounds **9** and **10**.

Scheme 2. Solid-Phase Synthesis of Peptide **9**, (4-Amino-3-iodo)-D-Phe-c[Cys-(3-iodo)-Tyr-D-Trp-Lys-Val-Cys]-Thr-NH₂



OH, was coupled to the peptide chain using DIC/HOBt (1:1 equiv) in DMF.

Biological Activity. The biological assays were carried out in the laboratories of Professor Steven W. J. Lamberts at University Hospital, Rotterdam, The Netherlands, by Joost van der Hoek, Peter M. van Koetsveld, and Leo J. Hofland. The binding assays were executed on membranes from cells transfected with individual human somatostatin receptor subtypes: CC531 cells (hsst2) and CHO-K1 cells (hsst1, hsst3, and hsst5). The functional assays (inhibition of GH and PRL secretion) were carried out with dispersed rat pituitary cells. The binding affinities for compounds **1–10** are shown in Table 2, and the functional assay results are shown in Table 3. The experimental details are found in the Experimental Section.

Conformational Analysis. NMR and Molecular Modeling Studies. These studies were carried out by Dr. Antonia de Capua. The structures of all the compounds were confirmed by 1D and 2D ¹H NMR in DMSO at 500 MHz.

Table 2. Binding Affinity to Receptors hsst2, hsst3, and hsst5 (IC₅₀ in nM)^a

peptide	receptors and IC ₅₀		
	hsst2	hsst3	hsst5
SS-14	0.4	0.4	0.2
octreotide	0.02	92.9	21.8
octreotide amide	0.79	> 50	8.4
1	18.6	> 1000	5.6
2	1.6	> 1000	14
3	11	> 1000	54
4	17	> 1000	3.4
5	1.1	> 1000	30
6	6.2	> 1000	1
7	1.4	> 1000	10
8	12	> 1000	74
9	0.63	> 1000	0.65
10	1.9	> 1000	2.9

^a Data were available for hsst1, when in all cases IC₅₀ was > 1000 nM.

(a) NMR Spectroscopy. The samples were dissolved in DMSO-*d*₆. The NMR spectra were acquired on a Bruker AMX 500 spectrometer operating at 500 MHz and processed using FELIX2000 (Biosym/MSI, Inc.).

The ¹H NMR data are presented in the Supporting Information as follows: Tables S1 and S2 (chemical shifts), Tables S3 and S4 (relevant backbone NOEs), and Tables S5 and S6 (coupling constants $J_{\text{NH}-\text{C}^{\alpha}\text{H}}$, calculated ϕ angles, coupling constants $J_{\text{C}^{\alpha}\text{H}-\text{C}^{\beta}\text{H}}/J_{\text{C}^{\alpha}\text{H}-\text{C}^{\beta}\text{Hh}}$, calculated side chain populations, and temperature coefficients). The following notations are observed: C^αH and H_α are used interchangeably to denote the proton linked to the α C atom. H_α³ denotes the proton linked to the α C atom of residue 3. The subscripts l and h denote low- and high-field resonances, respectively.

(b) Molecular Modeling. The computer simulations were carried out on an SGI IRIX 6.5 workstation and Challenge computer (Silicon Graphics). The Insight II and DISCOVER programs were used for the molecular mechanics, dynamics calculations, and visualizations.²⁰

Discussion

Our studies commenced with compound RC-121, D-Phe¹-c[Cys²-Tyr³-D-Trp⁴-Lys⁵-Val⁶-Cys⁷]-Thr⁸-NH₂, because of its binding profile, illustrated in Table 4, in comparison with native SS-14 and SS-28 and the synthetic analogue octreotide.^{21,22} The octapeptide RC-121 binds strongly to hsst2 and has a relatively high affinity to hsst5, but unlike octreotide, it does not bind to hsst3 in the nanomolar range.

We set out to modify residues in positions 1, 8, and 3 in RC-121. These modifications are based on previous work from our laboratory.^{22,23} Receptor–ligand complexes hsst2/L-363,301, hsst2/octreotide, and hsst5/octreotide were modeled (L-363,301 is a potent cyclic hexapeptide somatostatin analogue²⁴). The three complexes were very similar in the transmembrane region of the receptors. The β II' turn region (D-Trp-Lys) was inserted into the transmembrane region, while residues 1 and 8 in octreotide were in proximity of extracellular loop III (ECL III), which connects transmembrane helices VI and VII. Selectivity therefore arises from the fragments of the molecules interacting with ECL III. It was also determined that the electrostatic potentials of ECL III in hsst2 and hsst5 were different, corresponding to variations in amino acid sequences. While ECL III

Table 3. Functional Assays for **1–10**: Inhibition of GH and PRL Release from Rat Pituitary Cells^a

compound	% GH inhibition	% PRL inhibition	IC ₅₀ (nM)	
			GH	PRL
SS-14	66	30	0.1	0.2
[D-Phe ¹ -Asp ⁸], 1 ^b	nd	nd	1.1	nd
[(4-amino)-D-Phe ¹ -Thr ⁸], 2	47	20	0.08	2.2
[(4-amino)-D-Phe ¹ -Asp ⁸], 3	41	−9	14.8	26
[(4-amino)-D-Phe ¹ -D-Thr ⁸], 4	−11	8	nd	nd
[(4-amino)-D-Phe ¹ -D-Asp ⁸], 5	18	11	nd	>100
[(4-amino)-D-Phe ¹ -(3-iodo)-Tyr ³ -Thr ⁸], 6	12	14	nd	nd
[(4-amino-3-iodo)-D-Phe ¹ -Thr ⁸], 7	60	35	0.1	0.1
[(4-amino-3-iodo)-D-Phe ¹ -Asp ⁸], 8	17	12	nd	nd
[(4-amino-3-iodo)-D-Phe ¹ -(3-iodo)-Tyr ³ -Thr ⁸], 9	58	29	0.15	0.23
[(4-amino-3-iodo)-D-Phe ¹ -(3-iodo)-Tyr ³ -Asp ⁸], 10	55	15	nd	nd

^a nd: not determined. "IC₅₀ GH" represents the IC₅₀ of inhibition of GHRH-stimulated GH release. "IC₅₀ PRL" represents the IC₅₀ of inhibition of PRL release. ^b Compound **1** was tested separately, prior to series **2–10**, in comparison with octreotide, and only IC₅₀ for GH inhibition was available (octreotide IC₅₀ = 6.1 nM).

Table 4. Binding Affinities of Natural and Synthetic Somatostatin Analogues at hsst1–hsst5, K_i (nM) ± SEM^a

compound	hsst1	hsst2	hsst3	hsst4	hsst5
SS-14	2.3 ± 0.47	0.23 ± 0.04	1.17 ± 0.23	1.7 ± 0.3	1.4 ± 0.3
SS-28	2.4 ± 0.7	0.3 ± 0.06	1.27 ± 0.29	5.4 ± 2.6	0.4 ± 0.05
octreotide	875 ± 180	0.57 ± 0.08	26.8 ± 7.7	>1000	6.8 ± 1.0
RC-121	>1000	1.7 ± 0.5	>1000	>1000	13.1 ± 1.2

^a Data from Dr. John Taylor and Dr. Barry Morgan of Biomeasure, Inc.²²

of hsst2 was found to be mostly hydrophobic, the ECL III of hsst5 showed a combination of hydrophobicity and acidity. Compound Arg¹-c[Cys²-Tyr³-D-Trp⁴-Lys⁵-Val⁶-Cys⁷]-Lys⁸-NH₂ was found to be hsst5 selective (IC₅₀ = 24.7 nM). It was observed that in the hsst5/octreotide complex the hydrophobic part of ECL III interacted with D-Phe and Thr-ol while the acidic residues of ECLIII were kept away from the ligand. Hydrophobic residues bearing an amino group became attractive for further investigation in position 1, and we started with 4-amino-D-Phe-OH. We modified position 3 because it was an optimal site for introduction of iodine. We sought to obtain increased potency and selectivity at receptors hsst2 and hsst5. Moreover, by using unnatural amino acids, we expected to obtain compounds with increased half-lives. It is generally accepted that the resistance to enzymatic degradation of peptidomimetic compounds increases by introduction of unnatural amino acids.

Thus, we synthesized and characterized a series of analogues of RC-121. One of the compounds, D-Phe¹-c[Cys²-Tyr³-D-Trp⁴-Lys⁵-Val⁶-Cys⁷]-Asp⁸-NH₂ (**1**), denoted as [D-Phe¹-Asp⁸], bound with high affinity to receptors hsst2 and hsst5 (Table 2). The functional assay for compound [D-Phe¹-Asp⁸] (**1**), the inhibitory effect of this compound on GH release from rat pituitary cells, is presented in Table 3.

The biological results for [D-Phe¹-Asp⁸] (Tables 2 and 3) were highly encouraging. This compound was selective for hsst2 and hsst5 only, and in the in vitro test on rat pituitary cells, it was 5 times more potent than octreotide in inhibiting GH release. [Somatostatin receptors are divided into two separate subgroups based on differences in structure and, most importantly, pharmacological profile. Subgroup 1 (SRIF1) comprises sst2, sst3, and sst5, while subgroup 2 (SRIF2) includes sst1 and sst4. Octapeptides such as octreotide bind with high affinity to subgroup 1 but do not bind to subgroup 2 (see Table 4). Our compounds are structurally related to octreotide, therefore pharmacologically significant

binding to hsst1 and hsst4 was not expected. Binding data for hsst1 were available for compounds **1–10**, and in all cases IC₅₀ was >1000 nM. We are therefore confident of the selectivity of our compounds for hsst2 and hsst5.]

For the next generation of analogues (Table 1), we maintained residue 8 as Thr or Asp, both D- and L-isomers, and modified the D-Phe in position 1. We chose Asp as a modification for residue 8 on the basis of promising results for the compound [D-Phe¹-Asp⁸] (**1**). For modifications in position 1, the unnatural amino acid (4-aminomethyl)phenylalanine, which has the characteristics of both hydrophobicity and basicity, was prepared²² in our laboratory in the past, but the binding affinity of the peptide analogue that incorporated it was low. We replaced residue 1 with (4-amino)-D-Phe-OH in RC-121, giving D-Phe-c[Cys-Tyr-D-Trp-Lys-Val-Cys]-Thr-NH₂. The binding affinities and functional assay results for this group of target structures are presented in Tables 2 and 3, respectively.

Compounds with (4-amino)-D-Phe-OH in position 1 exhibited potent and selective binding at receptors hsst2 and hsst5. Compound [(4-amino)-D-Phe¹-Thr⁸] (**2**) was selective at the hsst2 receptor by an order of magnitude compared to the hsst5 receptor. It was also a modest inhibitor of GH and PRL release. In contrast, [(4-amino)-D-Phe¹-Asp⁸] (**3**), in which residue 8 was changed from Thr to Asp, lost binding affinity and caused an increase in PRL secretion, an undesirable effect. Compound [(4-amino)-D-Phe¹-D-Thr⁸] (**4**), where residue 8 was D-Thr, lost potency at the hsst2 receptor but interestingly gained potency at the hsst5 receptor. However, in the functional assay, [(4-amino)-D-Phe¹-D-Thr⁸] (**4**) actually increased GH release, an undesirable effect from the point of view of our aims in this study. Compound [(4-amino)-D-Phe¹-D-Asp⁸] (**5**) with D-Asp in position 8 was more selective at the hsst2 receptor than [(4-amino)-D-Phe¹-Thr⁸] (**2**) but had low functional activities.

To improve the binding affinities of our analogues, we turned our attention to iodination. It is well-known that radioiodination is a useful tool for the determination of tissue distribution of somatostatin receptors and for delivering toxic levels of radiation to somatostatin receptor-positive tumors, since several types of cancers express high densities of somatostatin receptors. Iodine has been extensively used for radiolabeling or chemical modification of peptides and proteins.^{25–29} Radioiodi-

nated analogues of hormones are used in binding assays for displacement studies (competitive binding assays).

There were several instances in the literature where iodination of opioid or somatostatin analogues produced interesting results, with an increase in binding affinity to receptors. Schiller et al.³⁰ monoiodinated the Tyr residue in the δ -opioid antagonist TIPP (H-Tyr-Tic-Phe-Phe-OH) and obtained a potent and selective δ -agonist. Rivier et al.³¹ obtained hsst1 receptor selective analogues, and monoiodination of Tyr caused an increase in potency compared to the noniodinated analogue (IC_{50} at hsst1 decreased from 17.1 ± 6.0 to 3.6 ± 0.7 nM). (This result was made public at the 17th American Peptide Symposium 2001, when we were already working on our iodinated analogues.) Woltering et al.³² obtained a series of N-terminally extended multiply tyrosinated somatostatin analogues (e.g., WOC4a, D-Tyr-Tyr-Tyr-D-Tyr-c[Cys-Phe-D-Trp-Lys-Thr-Cys]-Thr-NH₂), which maintained high affinity for somatostatin receptors, exhibited biological activity comparable to that of the native peptide, and retained all these characteristics after iodination. The analogues were radioiodinated to high specific activities and are applicable for tumor localization, scanning, and therapy.

We realized we had the possibility to create compounds that could be easily radioiodinated and be useful as agents for scintigraphy studies or vehicles for delivering toxic levels of radioactivity to tumors. Our peptides have two aromatic residues, Tyr and (4-amino)-D-Phe-OH. Peptides [(4-amino)-D-Phe¹-Thr⁸] (**2**), [(4-amino)-D-Phe¹-D-Thr⁸] (**4**), and [(4-amino)-D-Phe¹-D-Asp⁸] (**5**) had excellent binding affinity and selectivity for the hsst2 (**2** and **5**) and hsst5 (**4**) receptors (Table 2). Functionally, [(4-amino)-D-Phe¹-Thr⁸] (**2**) was the best lead compound, since it maintained the activity profile of SS-14 but at a slightly lower potency (GH release inhibition 47% and PRL inhibition 20%, Table 3). Therefore, for the next generation of modifications we focused on iodination of the residues with aromatic side chains. With use of monoiodinated building blocks **12** and **14**, several iodinated peptidomimetics were synthesized and characterized (Table 1).

We synthesized compound [(4-amino)-D-Phe¹-(3-iodo)-Tyr³-Thr⁸] (**6**), with an iodine on tyrosine, and [(4-amino-3-iodo)-D-Phe¹-Thr⁸] (**7**) with an iodine on 4-amino-D-phenylalanine. On the basis of good results for compound [D-Phe¹-Asp⁸] (**1**), we also included iodine in a compound with Asp in position 8 as in **1** to generate [(4-amino-3-iodo)-D-Phe¹-Asp⁸] (**8**). We were also interested in exploring the effect of two monoiodinated residues in the molecules. Thus, we prepared compounds [(4-amino-3-iodo)-D-Phe¹-(3-iodo)Tyr³-Thr⁸] (**9**) and (4-amino-3-iodo)-D-Phe¹-(3-iodo)Tyr³-Asp⁸] (**10**), the former with Thr in position 8 and the latter with Asp in position 8. We could then compare activities of target molecules with or without iodine and relate the biological activities (Tables 2 and 3) to their conformations.

Peptides [(4-amino-3-iodo)-D-Phe¹-Thr⁸] (**7**) and [(4-amino-3-iodo)-D-Phe¹-(3-iodo)-Tyr³-Thr⁸] (**9**) gave the best results. Both exhibited potent and selective binding for hsst2 and 5 receptors, as well as increased ability to inhibit both GH and PRL. Compound **7** is a substantial achievement. It showed high affinity to receptors hsst2 and 5 (EC_{50} values of 1.4 and 10 nM, respectively),

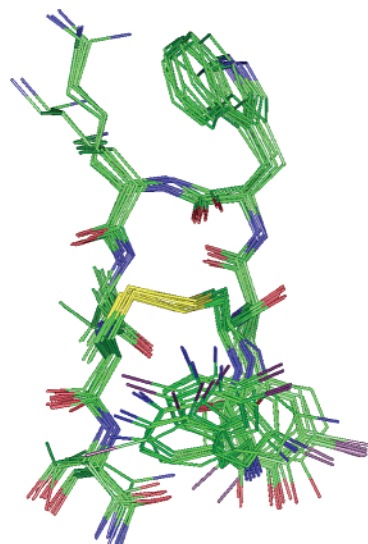


Figure 2. Trajectories from 5 ns of free molecular dynamics simulation of compound **9** at 300 K.

and it was inactive at receptors hsst1 and hsst3. Functionally, this compound inhibited GH (60%) and PRL (35%) comparably to SS-14 (66% and 30%, respectively). Compound [(4-amino-3-iodo)-D-Phe¹-(3-iodo)-Tyr³-Thr⁸] (**9**) represents a major breakthrough. It exhibits subnanomolar affinity to both hsst2 and hsst5 receptor subtypes, with EC_{50} of 0.63 and 0.65 nM, respectively, in the same nanomolar range as the EC_{50} values for SS-14 (0.4 and 0.2 nM, respectively). In the functional assays, compound [(4-amino-3-iodo)-D-Phe¹-(3-iodo)-Tyr³-Thr⁸] (**9**) inhibits stimulated GH release by 58% and PRL by 29%, comparable to somatostatin (66% and 30%, respectively).

The conformational analysis data show that the analogues studied have great similarity among each other, and when compared with octreotide (Figures 1 and 2). A more detailed description is found in the Supporting Information. The backbone conformation can be described as an antiparallel β -sheet containing a type II' β -turn around D-Trp-Lys. The disulfide bridge is a good mimetic of a β VI turn. In most analogues, the D-Phe¹ side chain adopted a trans conformation, which resulted in spatial proximity to the disulfide bridge. When the residues in position 8 were D-residues, the D-Phe¹ was oriented away from the disulfide bridge.

In the molecules containing iodine, there seemed to be a preference for the aromatic side chains to situate themselves close to one another (e.g., Figure 2). This tendency may create a large hydrophobic area, which may bind to a specific hydrophobic zone on the receptors. Alternatively, the presence of the large, hydrophobic iodine may induce a conformation that favors binding to receptors hsst2 and hsst5 but not to hsst3.

Conclusions

We synthesized potent somatostatin analogues selective for receptors hsst2 and hsst5, with inhibitory activity on GH and PRL comparable to that of somatostatin. Compound **9**, (4-amino-3-iodo)-D-Phe¹-c[Cys²-(3-iodo)-Tyr³-D-Trp⁴-Lys⁵-Val⁶-Cys⁷]-Thr⁸-NH₂, binds to receptors hsst2 and hsst5 with an EC_{50} of 0.63 and 0.65 nM, respectively, as potently as somatostatin. Functionally, this compound is also as potent as somatostatin.

It inhibits GH and PRL release by 58% and 29%, respectively, compared to 66% and 30% for somatostatin. The binding profile of our compounds is more refined than the one of octreotide, currently used in the clinic, because our compounds are selective at *hst2* and *hst5* only. The next step in this investigation will be to study the pharmacokinetics to assess the compounds' biological activity *in vivo*.

The analogues presented include major candidates, with possible future applications in detection and treatment of diseases that are difficult to treat, caused by hypersecretion of hormones (e.g., pituitary tumors, especially mixed GH–PRL releasing adenomas, and their side effects; diabetic retinopathy; cancers).

Experimental Section

General Notes. NMR spectra were obtained on a Varian HG-400 (400 MHz) and a Bruker AMX 500 (500 MHz) spectrometers. Chemical shifts (δ) are reported in parts per million (ppm) relative to residual undeuterated solvent as an internal reference. The following abbreviations were used to explain multiplicities: s = singlet, d = doublet, t = triplet, q = quartet, dd = doublet of doublets, m = multiplet, b = broad.

Optical rotations were recorded on a Perkin-Elmer 241 polarimeter.

IR spectra were recorded on a Nicolet-Magna-IR 550 series II spectrometer. Mass spectroscopic analyses (ESI, MALDI–FTMS) were carried out by the Scripps Center for Mass Spectrometry at The Scripps Research Institute, La Jolla, CA.

The target molecules were purified and analyzed by RP-HPLC using Vydac Protein Peptide C₁₈ columns. Column dimensions were 4.5 mm \times 250 mm (90 Å silica, 5 μ m) for analytical HPLC and were 22 mm \times 250 mm (90 Å silica, 10 μ m) for preparative HPLC. The UV absorbance was monitored at 220 nm (280 nm in some cases). A binary system of water (A) and acetonitrile (B), both containing 0.1% TFA, was used throughout. Preparative HPLC was carried out at 10 mL/min flow rate on two different instruments. One instrument was a system composed of two Waters 510 pumps and a dual wavelength UV absorbance detector. The other instrument, which was also used for analytical purposes as described below, was a Waters Millennium 2010 system, composed of two Waters 510 pumps, a 715 Ultra WISP sample injector, and a 996 photodiode array detector (PDA), operated by a NecStar PC compatible computer. Two analytical HPLC profiles of the pure compounds were obtained on the Waters Millennium PDA system, using a linear gradient of usually 10–90% acetonitrile (B) in water (A) over 30 min and an isocratic elution, both at 1 mL/min flow rate.

The following protected amino acids were used: Fmoc-Thr(*t*Bu)-OH, Fmoc-Asp(O*t*Bu)-OH, Fmoc-Cys(Acm)-OH, Fmoc-Val-OH, Fmoc-Lys(Boc)-OH, Fmoc-D-Trp(Boc)-OH, Fmoc-Tyr(*t*Bu)-OH, Boc-D-Phe-OH, available from Calbiochem-Novabiochem, a division of Merck, Darmstadt, Germany. The Rink amide MBHA resin and PyBOP were also purchased from Calbiochem-Novabiochem. Other reagents (coupling agents HBTU and DIC, H-(3-iodo)-Tyr-OH, Boc-(4-amino)-D-Phe-OH) were purchased from Chem-Impex International, Wood Dale, IL. The Boc-(4-Fmoc-amino)-D-Phe-OH was obtained from Bachem, Torrance, CA. The DMF was purchased from Fisher Scientific and treated with sodium aluminosilicate molecular sieves (4 Å nominal pore diameter) obtained from Sigma and Amberlite IR120 (plus) cation-exchange resin, strongly acidic. Methylene chloride (DCM) was distilled from calcium hydride. The reactions were monitored by thin-layer chromatography (TLC) carried out on EM Science Merck silica gel coated on aluminum plates (0.2 mm thickness, 60 F₂₅₄) using UV light (254 nm) as the visualizing agent and 10% ninhydrin in ethanol, bromocresol green in ethanol, or 7% ethanolic phos-

phomolybdic acid and heat as developing agents. Silica gel 60 (230–400 mesh) purchased from EM Science was used for column chromatography.

The Kaiser test³³ was used as a qualitative assay for the presence or absence of free amino groups during reactions on solid phase.

The peptides [(4-amino)-D-Phe¹-Thr⁸] (2), [(4-amino)-D-Phe¹-Asp⁸] (3), [(4-amino)-D-Phe¹-D-Thr⁸] (4), [(4-amino)-D-Phe¹-D-Asp⁸] (5), [(4-amino)-D-Phe¹-(3-iodo)-Tyr³-Thr⁸] (6), [(4-amino-3-iodo)-D-Phe¹-Thr⁸] (7), [(4-amino-3-iodo)-D-Phe¹-Asp⁸] (8), [(4-amino-3-iodo)-D-Phe¹-(3-iodo)-Tyr³-Thr⁸] (9), [(4-amino-3-iodo)-D-Phe¹-(3-iodo)-Tyr³-Asp⁸] (10) were constructed by manual solid phase synthesis methods, at a 0.2 mmol scale, using Rink amide MBHA resin with a substitution level of 0.54 mmol/g, using approximately 0.37 mg resin. The activation/coupling agents used were PyBOP/HOBt/DIEA, 4/4/8 (equiv), or HBTU/HOBt/DIEA, 4/4/8 (equiv). All couplings and deprotections were carried out in DMF. In some cases, NMP was also used. Generally, to couple the first amino acid, an amount of 5 equiv was used (5/5/10 equiv of FmocAA/coupling agent/DIEA), and the coupling reaction completed overnight. Then, 4 equiv of the commercially available amino acids were used, as above, and coupling reaction times were 4 to 8 h, allowing for differences in reactivity among amino acids. For coupling of cysteine, we chose an activation/coupling method that did not contain base, namely, DIC/HOBt, 1/1 (mmol), in a mixture of DCM/DMF 1/1 (vol), to minimize racemization. The reaction time was 2 h.

The resin was initially swollen in DCM for at least 30 min. Deprotection of the Fmoc group from the resin and throughout the synthesis was achieved with 20% piperidine in DMF. After deprotection, the peptide–resin was washed with 2 \times DMF for 1 min, then with 2 \times DCM, and then again with DMF (2 \times 1 min). After coupling, 4 \times 1 min DMF washes were followed by 2 \times DCM, then 2 \times MeOH, 2 \times DCM, and 4 \times DMF.

Cyclization was accomplished using excess I₂ (10 or 5 equiv) in DMF (20 mL) for 3 h. The peptide–resin was then washed 10 times with DMF, or more, until the solvent coming out of the reaction vessel was clear. To completely remove traces of iodine, a THF wash was followed by a 0.5 M Na₂S₂O₃ rinse, then DCM, MeOH, DCM, THF, and DMF. Finally, the peptide–resin was rinsed twice with DCM and dried in the desiccator under high vacuum.

For final deprotection of all side chain protecting groups and simultaneous cleavage of the peptide from the resin, a cocktail composed of 9.5 mL of TFA, 0.25 mL of H₂O, and 0.25 mL of anisole was used. The “cleavage cocktail” and the peptide–resin were separately cooled in ice. Then the solution was added over the resin and the vessel was shaken for 1 h at room temperature. The liquid was then filtered, and the resin was washed five times with neat TFA. The collected filtrate containing the final peptide as a TFA salt was evaporated to dryness, and traces of TFA were removed by coevaporation with toluene three times. The crude peptide was cooled in an ice bath, and cold ether was added, whereby a white precipitate formed. The precipitate was isolated by centrifugation followed by ether washes, then water was added, and the peptide was lyophilized overnight.

Peptide [D-Phe¹-Asp⁸] (1) was synthesized on an ABI 433A automated peptide synthesizer controlled by a Macintosh LC computer running ABI Synthasist software, version 2.0. All syntheses were performed using the FastMoc protocol, on a 0.1 mmol scale. Briefly, after DCM and NMP washes, the Fmoc protecting group on the Rink amide resin was deprotected using 20% piperidine in NMP two times, 2 min each. Monitoring of the conductivity of the deprotection solution and subsequent deprotection cycles were repeated until the conductivity value was within 10% of the previous deprotection. The first amino acid was coupled twice to ensure complete reaction. Couplings were carried out using 0.9 mmol of a 0.45 M HBTU/HOBt/NMP stock solution. The amino acid was dissolved in NMP and this solution and shaken for 6 min, after which 1 mL of a solution of 2 M DIEA was added. The coupling

Table 5. Summary of Experimental Data for Compounds **1–10**

peptide	analytical HPLC ^a	<i>t</i> _R (min)	formula	MH ⁺ , <i>m/z</i>	
				expected	found ^b
1	20–40	13.63	C ₅₀ H ₆₅ N ₁₁ O ₁₁ S ₂	1060.4379	1060.4414
	26	10.20			
2	10–90	14.33	C ₅₀ H ₆₈ N ₁₂ O ₁₀ S ₂	1061.4695	1061.4733
	26	11.13			
3	10–90	17.12	C ₅₀ H ₆₆ N ₁₂ O ₁₁ S ₂	1075.4488	1075.4448
	26	8.72			
4	10–90	13.58	C ₅₀ H ₆₈ N ₁₂ O ₁₀ S ₂	1061.4695	1061.4650
	20	11.59			
5	10–90	13.59	C ₅₀ H ₆₆ N ₁₂ O ₁₁ S ₂	1075.4488	1075.4492
	20	11.26			
6	10–90	18.04	C ₅₀ H ₆₇ IN ₁₂ O ₁₀ S ₂	1187.3662	1187.3780
	26	16.45			
7	10–90	18.90	C ₅₀ H ₆₇ IN ₁₂ O ₁₀ S ₂	1187.3662	1187.3689
	25	9.32			
8	10–90	18.74	C ₅₀ H ₆₅ IN ₁₂ O ₁₁ S ₂	1201.3454	1201.3542
	22	10.65			
9	10–90	20.40	C ₅₀ H ₆₆ I ₂ N ₁₂ O ₁₀ S ₂	1313.2628	1313.2644
	25	11.17			
10	10–90	17.62	C ₅₀ H ₆₄ I ₂ N ₁₂ O ₁₁ S ₂	1327.2421	1327.2423
	25	10.41			

^a Expressed as % B (see Experimental Section). ^b MALDI-FTMS. There is additional MN⁺ data for compounds **6–10** (see Experimental Section).

was carried out for 9 min, followed by successive NMP washes and capping with acetic anhydride. After the last amino acid was coupled, the terminal Fmoc was cleaved off with piperidine and the resin was washed four times with NMP and six times with DCM. The peptide–resin was then recovered and cyclization by disulfide bond formation was carried out, using 10 equiv of I₂ in 10 mL of DMF for 3 h. The final deprotection of side chain protecting groups and cleavage from the resin proceeded for 1 h in the presence of a “cleavage cocktail” consisting of 9.5 mL of TFA, 2.5 mL of H₂O, 2.5 mL of anisole, 0.1 mL of EDT, and 0.1 mL of phenol. The peptides were obtained as white or yellow-tinged solids after ether precipitation and lyophilization. A summary of analytical data for peptides **1–10** is presented in Table 5.

Synthesis of the Amino Acid Building Blocks. Fmoc-(3-iodo)-tyrosine (12) [2-(9H-Fluoren-9-ylmethoxycarbonylamino)-3-(4-hydroxy-3-iodophenyl)propionic Acid]. To H-(3-iodo)-Tyr-OH (1.00 g, 3.26 mmol) were added 7 mL of DMF and 10 mL of acetone, and the suspension was cooled to 0 °C in an ice bath. After 10 min, 10% NaHCO₃ (w/v) (7 mL, 8.15 mmol) was added dropwise, followed by FmocOSu (1.32 g, 3.91 mmol). Another 25 mL of DMF was added, and the milky suspension was stirred vigorously at room temperature, overnight. (Note: the starting material was insoluble in water, DMF, THF, dioxane, acetonitrile, acetone, CHCl₃, and DCM.) The solvent was removed under reduced pressure, and an amount of 25 mL of water was added. The water was extracted once with EtOAc (5 mL) to remove organic impurities. The aqueous layer was cooled in an ice bath and acidified to approximately pH 1 with 2 N NaHSO₄ and extracted five times with EtOAc (5 × 5 mL). The EtOAc layer was then washed twice with saturated NaCl, dried over Na₂SO₄, filtered, and concentrated to result in a clear oil. This was dried overnight on a vacuum manifold to become a white foamy solid. Chloroform (50 mL) was added, and a white precipitate formed. The precipitate (product) was filtered on a Buchner funnel and dried overnight to yield 1.41 g (82%). ¹H NMR (DMF, 400 MHz): δ (ppm) 7.87 (d, *J* = 8 Hz, 2H), 7.63 (t, *J* = 8 Hz, 2H), 7.57 (s, 1H), 7.39 (m, 2H), 7.33 (m, 2H), 7.06 (d, *J* = 8 Hz, 1H), 6.77 (d, *J* = 8 Hz, 1H), 4.18 (m, 3H), 4.02 (m, 1H), 2.94 (m, 1H), 2.72 (m, 1H). MS, ESI (*m/z*), calculated for C₂₄H₂₀NO₅I: [MH]⁺ expected 530, found 530; [M + Na]⁺ expected 552, found 552; [M – H][–] expected 528, found 528. [α]_D²⁵ +9.04° (*c* 0.88, MeOH). TLC (CHCl₃/MeOH/AcOH 90:10:1, bromocresol green), *R*_f = 0.33.

Boc-(4-amino-3-iodo)-D-Phe-OH (14). [3-(4-Amino-3-iodophenyl)-2-tert-butoxycarbonylamino-3-iodopropionic Acid].³⁴ To a 100 mL round-bottomed flask were added Boc-(4-amino)-

D-Phe-OH (300 mg, 1.070 mmol) and 5 mL of glacial acetic acid. The flask was covered in aluminum foil. While stirring, ICl (174 mg, 1.070 mmol) was added dropwise, and the flask was immediately capped. The reaction mixture was stirred for 10 min. An excess of 0.5 N Na₂S₂O₃ was added to stop the reaction and quench remaining unreacted iodine (the solution turned from brown to slightly yellow). Ethyl acetate and water were added, and the layers were separated. The aqueous layer was back-extracted twice with ethyl acetate. The combined organic layer was further washed with 0.5 N Na₂S₂O₃ (3 × 5 mL) and saturated NaCl (3 × 5 mL), dried over Na₂SO₄, and filtered. The filtrate was concentrated, and the residue was dried on a vacuum manifold. The crude was purified by column chromatography using as eluent EtOAc/hexanes/AcOH 50:50:1 (mL) to yield 118.4 mg of product (27%). A portion of the product was further purified by HPLC and lyophilized to provide a sample for analytical purposes (for conditions see below). ¹H NMR (DMSO, 400 MHz): δ 7.46 (s, 1H), 7.03 (d, *J* = 8.4 Hz, 1H), 6.99 (d, *J* = 8 Hz, 1H), 6.73 (d, *J* = 8 Hz, 1H), 3.96 (m, 1H), 2.83 (dd, *J*₁ = 16 Hz, *J*₂ = 4 Hz, 1H), 2.63 (dd, *J*₁ = 16 Hz, *J*₂ = 12 Hz, 1H), 1.32 (s, 9H). ¹³C NMR (DMSO, 400 MHz): δ 173.4, 155.1, 146.6, 138.5, 129.6, 127.3, 113.9, 82.9 (C–I), 77.9, 55.4, 34.9, 28.2. MS ESI (*m/z*) calculated for C₁₄H₁₉N₂O₄I: [MH]⁺ expected 407, found 407; [M + Na]⁺ expected 429, found 429; [M – H][–] expected 405, found 405. MALDI-FTMS: [M + Na]⁺ expected 429.0282, found 429.0290. Mp 68–80 °C (with decomposition). [α]_D²⁵ –27.5° (*c* 1, MeOH) (starting material [α]_D²⁵ –26.9°, *c* 1, MeOH). TLC (EtOAc/hexanes/AcOH 5:5:0.1 mL, ninhydrin) *R*_f = 0.36. HPLC analytical: 1 mg/mL sample concentration, 10 μL injection, 10–90% B (A = H₂O with 0.1% TFA v/v; B = AcCN with 0.1% TFA v/v) at 1 mL/min over 30 min, λ = 220 nm, *t*_R = 18.81 min. The starting material in the same conditions exhibited an *t*_R = 12.16 min.

Synthesis of the Peptides. D-Phe-c[Cys-Tyr-D-Trp-Lys-Val-Cys]-Asp-NH₂ (1) was synthesized on the ABI 433A peptide synthesizer, as described in the general experimental procedures, using a Rink amide resin, 0.54 mmol/g, 0.1 mmol, 0.1852 g of resin. Cyclization was allowed to proceed for 4 h with 20 equiv of I₂ in 10 mL of DMF. The crude yield was 120.9 mg, out of which 43.1 mg of pure peptide were obtained, 41% overall. Purification was achieved with 20–50% B over 30 min (10 mL/min, λ = 220 nm) or with 26% B isocratic. The purity of the compound was ascertained by analytical HPLC on the PDA system, using a gradient of 20–40% B, *t*_R = 13.63 min and isocratic elution with 26% B, *t*_R = 10.29 min. MALDI-FTMS (*m/z*): [MH]⁺ calcd for C₅₀H₆₅N₁₁O₁₁S₂ expected 1060.4379, found 1060.4414.

(4-Amino)-D-Phe-c[Cys-Tyr-D-Trp-Lys-Val-Cys]-Thr-NH₂ (2) was synthesized by manual SPPS, on Rink amide resin (substitution level 0.54 mmol/g), 0.2 mmol scale, to yield 228 mg of crude peptide. A portion of the product was purified using 25% B at $\lambda = 280$ nm to yield 16.9 mg of pure peptide. Analytical conditions were the following: gradient 10–90% B, $t_R = 14.33$ min and isocratic 26% B, $t_R = 11.13$ min. MALDI-FTMS (m/z): [MH]⁺ calcd for C₅₀H₆₈N₁₂O₁₀S₂ expected 1061.4695, found 1061.4733.

(4-Amino)-D-Phe-c[Cys-Tyr-D-Trp-Lys-Val-Cys]-Asp-NH₂ (3) was synthesized by manual SPPS on Rink amide MBHA resin (0.54 mmol/g), 0.37 g, 0.2 mmol scale, as noted above. The crude yield was 143.8 mg. A portion of the peptide (40 mg) was purified with 25% B isocratic at $\lambda = 280$ nm to yield 13.3 mg of pure peptide. Analytical conditions were the following: gradient 10–90% B over 30 min, $t_R = 17.12$ min and isocratic 26% B, $t_R = 8.72$ min. MALDI-FTMS (m/z): [MH]⁺ calcd for C₅₀H₆₆N₁₂O₁₁S₂ expected 1075.4488, found 1075.4448.

(4-Amino)-D-Phe-c[Cys-Tyr-D-Trp-Lys-Val-Cys]-D-Thr-NH₂ (4) was synthesized as noted above, on 0.1 mmol scale, and 115 mg of crude was obtained. Purification of a portion of material was carried out using isocratic conditions of 23% B at $\lambda = 220$ nm, and an amount of 5 mg of pure product was obtained. Analytical conditions were the following: gradient 10–90% B over 30 min, $t_R = 13.58$ min and isocratic 20% B, $t_R = 11.59$ min. MALDI-FTMS (m/z): [MH]⁺ calcd for C₅₀H₆₈N₁₂O₁₀S₂ expected 1061.4695, found 1061.4650.

(4-Amino)-D-Phe-c[Cys-Tyr-D-Trp-Lys-Val-Cys]-D-Asp-NH₂ (5) was synthesized manually, as noted above, on a Rink amide MBHA resin (0.54 mmol/g), 0.19 g, 0.1 mmol scale, and 88.9 mg was obtained. A portion of the peptide was purified using isocratic conditions (20% B) at $\lambda = 220$ nm, and 6.16 mg of pure peptide was obtained. Analytical HPLC conditions were the following: gradient 10–90% B over 30 min, $t_R = 13.59$ min, and isocratic 20%, $t_R = 11.26$ min. MALDI-FTMS (m/z): [MH]⁺ calcd for C₅₀H₆₆N₁₂O₁₁S₂ expected 1075.4488, found 1075.4492.

(4-Amino)-D-Phe-c[Cys-(3-iodo)-Tyr-D-Trp-Lys-Val-Cys]-Thr-NH₂ (6) was synthesized by manual SPPS, 0.2 mmol scale, 0.37 g of resin. Fmoc-(3-I)-Tyr-OH (0.26 g, 0.5 mmol, 2.5 equiv), PyBOP (0.26 g, 0.5 mmol, 2.5 equiv), HOBT (0.07 g, 0.5 mmol, 2.5 equiv), and DIEA (0.17 mL, 1.0 mmol, 5 equiv) were mixed in DMF (20 mL) and added over the deprotected peptide–resin. The resulting mixture was opalescent because the amino acid was not completely soluble. Despite this problem, the coupling of this building block was successful. The resin was moved from the reaction vessel into a scintillation vial, and coupling was carried out overnight. The resin was removed from the scintillation vial, washed in a Buchner funnel several times with DMF and DCM, and then transferred back to the reaction vessel for subsequent couplings. The Kaiser test was used to assess the completion of the reaction, and the resin was washed again with DMF (4 × 20 mL), DCM (2 × 20 mL), and DMF (4 × 20 mL). The building of the peptide chain was resumed as usual. The last amino acid added was Boc-(4-Fmoc-amino)-D-Phe-OH (0.25 g, 0.5 mmol, 2.5 equiv) preactivated in the presence of PyBOP (0.42 g, 0.5 mmol, 2.5 equiv), HOBT (0.12 g, 0.5 mmol, 2.5 equiv), and DIEA (0.21 mL, 0.5 mmol, 5 equiv), in 20 mL of DMF. This residue was coupled for 18 h. For cyclization, only 5 equiv of iodine (0.25 g, 1.0 mmol) was used, for 3 h, to prevent iodination of the aromatic residues. The peptide–resin was then extensively washed as described in General Notes and dried for 2 h in a desiccator under high vacuum to eliminate the smallest trace of iodine. The side chain Fmoc protecting group was removed using 20% piperidine in DMF, for 1 h. The peptide–resin was washed thoroughly and dried in a desiccator overnight in preparation for final deprotection/cleavage from the resin. Final treatment with TFA/H₂O/anisole (9.5/2.5/2.5 mL) and usual workup resulted in 237.7 mg of crude peptide. A portion of 23 mg of the crude product was purified using isocratic conditions, 25% B, $\lambda = 210$ and 220 nm, to yield 8.1 mg of pure product. Analytical conditions were the following: gradient 10–90% B, 30 min, $t_R = 18.04$ min, isocratic 26%

B, $t_R = 16.45$ min. MALDI-FTMS (m/z): [MH]⁺ calcd for C₅₀H₆₇IN₁₂O₁₀S₂ expected 1187.3662, found 1187.378; [M + Na]⁺ expected 1209.3481, found 1209.3533.

(4-Amino-3-iodo)-D-Phe-c[Cys-Tyr-D-Trp-Lys-Val-Cys]-Thr-NH₂ (7) was built as noted above, on 0.2 mmol scale, but only an amount of 90 mg of peptide–resin was used to couple the last amino acid. The coupling mixture contained Boc-(4-amino-3-iodo)-D-Phe-OH (0.044 g, 0.11 mmol, 1.5 equiv), DIC (0.017 mL, 0.11 mmol, 1.5 equiv), and HOBT (0.017 g, 0.11 mmol, 1.5 equiv) in 10 mL of DMF, and the reaction was allowed to proceed for 10 h. Cyclization was carried out with iodine (0.16 g, 2.0 mmol, 10 equiv) for 3 h, and the peptide–resin was carefully washed and dried. The final deprotection/cleavage procedure was accomplished in 1 h, and after lyophilization, 30.6 mg of crude peptide resulted. Purification was accomplished with 24% B in isocratic mode. The yield was 9.9 mg (13% based on theoretical loading level of the resin). Analytical HPLC conditions were as follows: gradient 10–90% B, $\lambda = 220$ nm, $t_R = 18.9$ min, isocratic 25% B, $t_R = 9.32$ min. MALDI-FTMS (m/z): [MH]⁺ calcd for C₅₀H₆₇IN₁₂O₁₀S₂ expected 1187.3662, found 1187.3689; [M + Na]⁺ expected 1209.3481, found 1209.3470.

(4-Amino-3-iodo)-D-Phe-c[Cys-Tyr-D-Trp-Lys-Val-Cys]-Asp-NH₂ (8) was synthesized as above. A portion of 90 mg of peptide–resin was used for coupling of the final building block, which resulted in 19.4 mg of crude peptide. The peptide was purified with 24% B at $\lambda = 220$ nm. The yield was 4.1 mg (7% overall). Analytical HPLC conditions were as follows: gradient 10–90% B, 30 min, $t_R = 18.74$ min and isocratic 22% B, $t_R = 10.65$ min. MALDI-FTMS (m/z): [MH]⁺ calcd for C₅₀H₆₅IN₁₂O₁₁S₂ expected 1201.3454, found 1201.3542; [M + Na]⁺ expected 1223.3274, found 1223.3296.

(4-Amino-3-iodo)-D-Phe-c[Cys-(3-iodo)-Tyr-D-Trp-Lys-Val-Cys]-Thr-NH₂ (9) was synthesized as above, using 90 mg of peptide–resin. The couplings of the unusual building blocks were carried out as described above. The crude yield was 41 mg. Purification was carried out with 25–50% B over 30 min at $\lambda = 220$ nm. The yield was 4.1 mg (7.4% overall). Analytical conditions were as follows: gradient 10–90% B, 30 min, $t_R = 20.4$ min and isocratic 25% B, $t_R = 11.17$ min. MALDI-FTMS (m/z): [MH]⁺ calcd for C₅₀H₆₆I₂N₁₂O₁₀S₂ expected 1313.2628, found 1313.2644; [M + Na]⁺ expected 1335.2448, found 1335.2471.

(4-Amino-3-iodo)-D-Phe-c[Cys-(3-iodo)-Tyr-D-Trp-Lys-Val-Cys]-Asp-NH₂ (10) was synthesized by manual SPPS as described above, and an amount of 38.7 mg of crude was obtained. Purification conditions were as follows: 25–40% B, 30 min, $\lambda = 220$ nm. The yield was 5 mg (7.8% overall). Analytical conditions were as follows: gradient 10–90% B over 40 min, $t_R = 17.62$ min, isocratic 25% B, $t_R = 10.41$ min. MALDI-FTMS (m/z): [MH]⁺ calcd for C₅₀H₆₄I₂N₁₂O₁₁S₂ expected 1327.2421, found 1327.2423; [M + Na]⁺ expected 1349.224, found 1349.2274.

Biological Testing. The biological assays were carried out in the laboratories of Professor Steven W. J. Lamberts at University Hospital, Rotterdam, The Netherlands, by Joost van der Hoek, Peter M. van Koetsveld, and Leo J. Hofland. The binding assays were executed on membranes from CC531 cells (hsst2) and CHO-K1 cells (hsst1, hsst3, and hsst5), transfected with individual human somatostatin receptor subtypes. The functional assays (inhibition of GH and PRL secretion) were carried out with dispersed rat anterior pituitary cells. The results are presented in the text above, and the experimental details are found below.

Animals. Female Wistar rats (Harlan, The Netherlands), weighing 180–200 g, were kept in an artificially illuminated room (08.30 to 20.30 h) with food and water ad libitum. The animals were killed between 09.00 and 10.00 h by decapitation. The pituitary glands were removed within 5 min after killing, the neurointermediate lobe was discarded, and the anterior lobes were collected in calcium and magnesium Hank's balanced salt solution (HBSS) supplemented with 1% human serum albumin (HSA), penicillin (100 U/mL), streptomycin

(100 $\mu\text{g/mL}$), fungizone (0.5 $\mu\text{g/mL}$), and sodium carbonate (0.4 g/L final concentration).

Rat Anterior Pituitary Cell Culture. Female anterior pituitary cells were isolated with dispase as described in detail elsewhere.³⁵ The dispersed cells were seeded at a density of $(0.5\text{--}5) \times 10^5$ cells per well in multiwell plates. The culture medium was Eagle's minimum essential medium with Earle's salts supplemented with nonessential amino acids, 1 mM sodium pyruvate, 2 mM L-glutamine, penicillin (100 U/mL), streptomycin (100 $\mu\text{g/mL}$), fungizone (0.25 $\mu\text{g/mL}$), sodium bicarbonate (2.2 g/L final concentration), and 10% fetal calf serum (Invitrogen, Breda, The Netherlands). Media and supplements were obtained from Gibco Bio-Cult Europe (Invitrogen, Breda, The Netherlands). The cells were allowed to attach for at least 3 days. Thereafter, the medium was changed, 4 h incubations without or with the SS analogues were administered, and 10 nM GH-releasing hormone (GHRH) in 1 mL of complete culture medium was initiated, using four dishes for every treatment group. The results of each experiment were expressed as the percentage change of hormone release compared with control untreated dishes. The concentrations of rat GH and PRL were determined by means of a commercially available rat GH and PRL assay (Amersham, U.K.).

Somatostatin Receptor Transfection. For expression of the somatostatin receptor subtype sst2 and sst1, sst3, sst5 in rat colon carcinoma (CC531) cells and Chinese hamster ovary (CHO)-K1 cells, respectively, human sst1, sst2, sst3, or sst5 cDNA in pBluescript (pBS) (a kind gift of G. I. Bell, Howard Hughes Medical Institute Chicago, IL) was excised from pBS and inserted into the Nhe-1/SalI cloning site of the retroviral expression vector pCi-neo. The selection was made by the geneticine resistance gene (G418). This vector was used to stably transfect (using DOTAP) CC531 and CHO-K1 cells. Stably transfected CC531 and CHO-K1 cells were selected and cultured in RPMI 1640 medium and nutrient mixture F12 (HAM) medium [both supplemented with penicillin (100 U/mL), streptomycin (100 $\mu\text{g/mL}$), fungizone (0.25 $\mu\text{g/mL}$), and 10% FCS + geneticine (0.5 mg/mL)], respectively.

Receptor Binding Studies. Competitive binding experiments were performed with membranes prepared from CC531 (sst2) and CHO-K1 (sst1, sst3, sst5) cells expressing the respective human somatostatin receptor subtype. The method of membrane isolation, and the reaction conditions were the same as described previously.³⁶ Briefly, membrane preparations (corresponding to 25–50 μg of protein) of cultured cells were incubated in a total volume of 100 μL at room temperature for 45 min with 40,000 cpm [¹²⁵I]-labeled [Tyr¹¹]somatostatin-14 (2000 Ci/mmol) in the presence of increasing amounts of unlabeled SRIF analogues. At the end of the incubation time, 1 mL ice-cold Hepes buffer (10 mM Hepes, 5 mM MgCl₂, and 0.02 g/L bacitracin, pH 7.6) was added, and membrane-bound radioactivity was separated from unbound by centrifugation during 2 min at 14 000 rpm in an Eppendorf microcentrifuge. The remaining pellet was washed in ice-cold Hepes buffer, and the final pellet was counted in a γ -counter. Specific binding was defined as the total amount of radioligand bound minus that bound in the presence of 1 μM unlabeled SRIF analogue.

Statistical Analysis. The statistical significance of the difference between mean values was determined using one-way analysis of variance (ANOVA). When significant overall effects were obtained by this method, comparisons were made using Newman–Keuls multiple comparison test. Data are expressed as mean \pm SEM. A *P* value less than 0.05 was considered statistically significant. Calculation of the IC₅₀ values for displacement of [¹²⁵I]-labeled [Tyr¹¹]somatostatin-14 was performed using the GraphPad Prism (San Diego, CA) computerized program.

NMR Spectroscopy. The resonance assignments were carried out using ¹H NMR, TOCSY (total correlation spectroscopy),^{37–40} and ROESY (rotating frame nuclear Overhauser spectroscopy)⁴¹ experiments. A detailed description is found in the Supporting Information.

Molecular Modeling. Initially, 200 structures were generated using DGII/InsightII, followed by a restrained minimization with a CVFF91 force field and the Newton–Raphson VA09A algorithm with a convergence criterion of 0.001 kcal mol^{−1} Å^{−1}. All the calculations were carried out in vacuo, and a distance-dependent dielectric constant was used to take into account the solvent effects.⁴² In the simulations, the peptide bonds were maintained in the trans conformation.

The torsion angles, the NOE distances, and hydrogen-bonding patterns of these structures were compared with the values derived from NMR measurements. A Karplus-type equation was used to compute the torsion angles consistent with the measured *J*_{NH–C^αH} coupling constants, and an error of $\pm 30^\circ$ was tolerated. In the case of selections based on the hydrogen bonds, structures were retained in which NH protons with a temperature coefficient greater than 2.0 –ppb/K were considered to be involved in a hydrogen bond. Structures not consistent with these experimental constraints were discarded. A cutoff of 10 kcal/mol above the lowest energy conformer was used to sort out unrealistically high-energy conformations of the remaining structures.

A cluster analysis was performed by first extracting the lowest energy conformer out of all the conformations under investigation. These conformers served as a “seed” to grow a cluster as long as the selected torsion was within a 30° interval. The analysis then iteratively searched for the next high-energy cluster until the highest family was found. Prior to every molecular dynamics simulation, the system was equilibrated with 3 ps of initialization dynamics. In attempts to carry out a thorough search of the accessible conformational space, the lowest energy conformation of the clusters was subjected to 500 ps of restrained molecular dynamics at 1000 K with a step size of 1 fs. The conformers that were consistent with experimental data were subjected to the same cluster analysis as described above. Finally, the lowest energy structure of each cluster was chosen as the preferred conformation in solution of the somatostatin analogues.⁴³ Unrestrained molecular dynamics simulations at 300 K with a distance-dependent dielectric constant of 1 were carried out to investigate the equilibrium between these preferred conformations. The selected conformers were first submitted to 3 ps of equilibrium, followed by a step size of 1 fs for a 5 ns simulation. Structures were collected every 10 ps. During this process, conformational interchanges were observed.

Acknowledgment. We gratefully acknowledge the NIH-DK 15410 grant for financial support. Our deep gratitude is extended to Elisabetta Bosa, Mara Fabbri, and Lotte Hansen (in alphabetical order) for their support, vast IT knowledge, and help in presenting the Supporting Information. We also thank Joseph Taulane and Robyn Swanland for their contributions in publishing this manuscript.

Supporting Information Available: Tables of NMR data for all final peptides, experimental NMR details and discussion, figures of preferred conformational clusters for all peptides, spectra, and HPLC chromatograms for representative compounds. This material is available free of charge via the Internet at <http://pubs.acs.org>.

References

- (1) Brazeau, P.; Vale, W.; Burgus, R.; Ling, N.; Butcher, M.; et al. Hypothalamic Peptide That Inhibits the Secretion of Immunoreactive Pituitary Growth Hormone. *Science* **1973**, *179*, 77–79.
- (2) Pradayrol, L.; Joernvall, H.; Mutt, V.; Ribert, A. N-Terminally Extended Somatostatin. The Primary Structure of Somatostatin-28. *FEBS Lett.* **1980**, *109*, 55–58.
- (3) Epelbaum, J. Somatostatin in the Central Nervous System: Physiology and Pathological Modifications. *Prog. Neurobiol.* **1986**, *27*, 63–100.
- (4) Gomez-Pan, A.; Reed, J.; Albinus, M.; Shaw, B.; Hall, R.; et al. Direct Inhibition of Gastric Acid and Pepsin Secretion by Growth Hormone Release-Inhibiting Hormone in Cats. *Lancet* **1975**, *1*, 888–893.

- (5) Hellman, B.; Lernmark, A. Inhibition of the in Vitro Secretion of Insulin by an Extract of Pancreatic α_1 Cells. *Endocrinology* **1969**, *84*, 1484–1488.
- (6) Reichlin, S. Somatostatin. *N. Engl. J. Med.* **1983**, *309*, 1495–1563.
- (7) Reisine, T. Somatostatin. *Cell. Mol. Neurobiol.* **1995**, *15*, 597–614.
- (8) Meyerhof, W. The Elucidation of Somatostatin Receptor Functions: A Current View. *Rev. Physiol., Biochem. Pharmacol.* **1998**, *133*, 55–108.
- (9) Patel, Y. C. Somatostatin and Its Receptor Family. *Front. Neuroendocrinol.* **1999**, *20*, 157–198.
- (10) Reisine, T.; Bell, G. I. Molecular biology of somatostatin receptors. *Endocr. Rev.* **1995**, *16*, 427–442.
- (11) Lamberts, S. W. J.; Krenning, E. P.; Reubi, J. C. The Role of Somatostatin and Its Analogues in the Diagnosis and Treatment of Tumors. *Endocr. Rev.* **1991**, *12*, 450–482.
- (12) Hofland, L. J.; Lamberts, S. W. J. The Pathophysiological Consequences of Somatostatin Receptor Internalization and Resistance. *Endocr. Rev.* **2003**, *24*, 28–47.
- (13) Shimon, I.; Taylor, J. E.; Dong, J. Z.; Bitonte, R. A.; Kim, S.; et al. Somatostatin Receptor Subtype Specificity in Human Fetal Pituitary Cultures. *J. Clin. Invest.* **1997**, *99*, 789–798.
- (14) Shimon, I.; Yan, X.; Taylor, J. E.; Weiss, M. H.; Culler, M. D.; et al. Somatostatin Receptor (SSTR) Subtype-Selective Analogues Differentially Suppress in Vitro Growth Hormone and Prolactin in Human Pituitary Adenomas. *J. Clin. Invest.* **1997**, *100*, 2386–2392.
- (15) Saveanu, A.; Gunz, G.; Dufour, H.; Caron, P.; Fina, F.; et al. BIM-23244, a Somatostatin Receptor Subtype 2- and 5-Selective Analog with Enhanced Efficacy in Suppressing Growth Hormone (GH) from Octreotide-Resistant Human GH-Secreting Adenomas. *J. Clin. Endocrinol. Metab.* **2001**, *86*, 140–145.
- (16) Freda, P. U. Clinical review 150: somatostatin analogs in acromegaly. *J. Clin. Endocrinol. Metab.* **2002**, *87*, 3013–3018.
- (17) Scarpignato, C.; Pelosini, I. Somatostatin Analogs for Cancer Treatment and Diagnosis: An Overview. *Chemotherapy* **2001**, *47*, 1–29.
- (18) Molitch, M. E. *The Pituitary*; Blackwell Science Inc.: Cambridge, MA, 1995; pp 443–477.
- (19) Rohrer, S. P.; Birzin, E. T.; Mosley, R. T.; Berk, S. C.; Hutchins, S. M.; et al. Rapid Identification of Subtype-Selective Agonists of the Somatostatin Receptors through Combinatorial Chemistry. *Science* **1998**, *282*, 737–740.
- (20) Discover, version 3.0; Biosym/MSI: San Diego, CA.
- (21) Cai, R. Z.; Szoke, B.; Lu, R.; Fu, D.; Redding, T. W.; et al. Synthesis and Biological Activity of Highly Potent Octapeptide Analogs of Somatostatin. *Proc. Natl. Acad. Sci. U.S.A.* **1986**, *83*, 1896–1900.
- (22) Li, H. *Design and Synthesis of Peptidomimetic Building Blocks and Bioactive Molecules*; University of California, San Diego: San Diego, CA, 1998.
- (23) Jiang, X. *Computational and NMR Studies of Biologically Active Molecules*; University of California, San Diego: San Diego, CA, 1998.
- (24) Veber, D. F.; Freidinger, R. M.; Schwenk Perlow, D.; Paleveda, W. J.; Holly, F. W.; et al. A Potent Cyclic Hexapeptide Analogue of Somatostatin. *Nature* **1981**, *292*, 55–58.
- (25) Greenwood, F. C.; Hunter, W. M. The Preparation of ^{131}I -Labelled Human Growth Hormone of High Specific Radioactivity. *Biochem. J.* **1963**, *89*, 114–123.
- (26) Seevers, R. H.; Counsell, R. E. Radioiodination Techniques for Small Organic Molecules. *Chem. Rev.* **1982**, *82*, 575–590.
- (27) Tsomides, T. J.; Eisen, H. N. Stoichiometric Labeling of Peptides by Iodination on Tyrosil and Histidyl Residues. *Anal. Biochem.* **1993**, *210*, 129–135.
- (28) Vazquez, J.; Feigenbaum, P.; Katz, G.; King, V. F.; Reuben, J. P.; et al. Characterization of High Affinity Binding Sites for Charybdotoxin in Sarcolemmal Membranes from Bovine Aortic Smooth Muscle. *J. Biol. Chem.* **1989**, *264*, 20902–20909.
- (29) Kozlowski, E. S.; Johnson, G.; Dischino, D.; Dworetzky, S. I.; Boissard, C. G.; et al. Synthesis and Biological Evaluation of an Iodinated Iberiotoxin Analogue, [Mono-iodo-Tyr⁵, Phe³⁶]-iberiotoxin. *Int. J. Pept. Protein Res.* **1996**, *48*, 194–199.
- (30) Lee, P. H.-K.; Nguyen, T. M.-D.; Chung, N. N.; Schiller, P. W.; Chang, K.-J. Tyrosine-Iodination Converts the δ -Opioid Peptide Antagonist TIPP to an Agonist. *Eur. J. Pharmacol.* **1995**, *280*, 211–214.
- (31) Rivier, J. E.; Hoeger, C.; Erchevgy, J.; Gulyas, J.; DeBoard, R.; et al. Potent Somatostatin Undecapeptide Agonists Selective for Somatostatin Receptor 1 (sst1). *J. Med. Chem.* **2001**, *44*, 2238–2246.
- (32) Woltering, D. A.; O'Dorisio, M. S.; Murphy, W. A.; Chen, F.; Drouant, G. J.; et al. Synthesis and Characterization of Multiply-Tyrosinated, Multiply-Iodinated Somatostatin Analogs. *J. Peptide Res.* **1999**, *53*, 201–213.
- (33) Kaiser, E.; Colescott, R. L.; Bossinger, C. D.; Cook, P. I. Color Test for Detection of Free Terminal Amino Groups in the Solid Phase Synthesis of Peptides. *Anal. Biochem.* **1970**, *34*, 595–598.
- (34) Eberle, A.; Schwyzler, R. Synthese von [D-Alanin¹, 4-azido-3',5'-ditritio-L-phenylalanin², norvalin⁴]- α -melanotropin als "Photoaffinitätsprobe" für Hormon-Rezeptor-Wechselwirkungen (Synthesis of D-Alanin¹, 4-azido-3',5'-ditritio-L-phenylalanin², norvalin⁴]- α -melanotropin as "Photoaffinity Probe" for Hormone-Receptor Interactions). *Helv. Chim. Acta* **1976**, *59*, 2421–2431.
- (35) Oosterom, R.; Blaauw, G.; Singh, R.; Verleu, T.; Lamberts, S. W. J. Isolation of Large Numbers of Dispersed Human Pituitary Adenoma Cells Obtained by Aspiration. *J. Endocrinol. Invest.* **1984**, *7*, 307–311.
- (36) Hofland, L. J.; Van Koetsveld, P. M.; Wouters, N.; Waaijers, M.; Reubi, J. C.; et al. Dissociation of Antiproliferative and Antihormonal Effects of the Somatostatin Analog Octreotide on 7315b Pituitary Tumor Cells. *Endocrinology* **1992**, *131*, 571–577.
- (37) Bax, A.; Mehlkopf, A. F.; Smidt, J. A Fast Method for Obtaining 2D J-Resolved Absorption Spectra. *J. Magn. Reson.* **1980**, *40*, 213–219.
- (38) Bodenhausen, G.; Vold, R. L.; Vold, R. R. Multiple Quantum Spin-Echo Spectroscopy. *J. Magn. Reson.* **1980**, *B37*, 93–106.
- (39) Davis, D. G.; Bax, A. Assignment of Complex ^1H NMR Spectra via Two-Dimensional Homonuclear Hartmann-Hahn Spectroscopy. *J. Am. Chem. Soc.* **1985**, *107*, 2820–2821.
- (40) Levitt, M. H.; Freeman, R.; Frekiel, T. Broadband Heteronuclear Decoupling. *J. Magn. Reson.* **1982**, *47*, 328–330.
- (41) Bothner-By, A. A.; Stephens, R. L.; Lee, J.; Warre, C. D.; Jeanloz, R. W. Structure Determination of a Tetrasaccharide: Transient Nuclear Overhauser Effects in the Rotating Frame. *J. Am. Chem. Soc.* **1984**, *106*, 811–813.
- (42) McCammon, J. A.; Wolynes, P. G.; Karplus, M. Picosecond Dynamics of Tyrosine Side Chains in Proteins. *Biochemistry* **1979**, *18*, 927.
- (43) Melacini, G.; Zhu, Q.; Goodman, M. Multiconformational NMR Analysis of Sandostatin (Octreotide): Equilibrium Between β -Sheet and Partially Helical Structures. *Biochemistry* **1997**, *36*, 1233–1241.

JM050376T